Uncertainty analysis of time resolved transmittance characterization of solid tissue phantoms

Jean-Pierre Bouchard*, Israël Veilleux, Isabelle Noiseux, Sébastien Leclair, Rym Jedidi, Michel Fortin and Ozzy Mermut

Institut national d'optique, 2740 Einstein, Québec, Qc, Canada G1P 4S4;

ABSTRACT

Solid tissue phantom are the preferred tool for the development, validation, testing and calibration of photon migration instrument. Accuracy, or trueness, of the optical properties of reference phantoms is of the utmost importance as they will be used as the conventional true value against which instrument errors will be evaluated. A detailed quantitative analysis of the uncertainty of time-resolved transmittance characterization of solid optical tissue phantom is presented. Random error sources taken into account are Poisson noise of the photon counting process, additive dark count noise and instrument response function stability. Systematic error sources taken into account are: phantom thickness uncertainty, refractive index uncertainty, time correlated single photon counting system time base calibration uncertainty. Correction procedures for these systematic errors are presented whenever a correction is possible.

Keywords: Scattering, tissue optics, spectroscopy, tomography, molecular imaging

1.   INTRODUCTION

Reference tissue phantoms are a mandatory tool in the development of a new diffuse spectroscopy application or in the calibration and quality control of instrument in use [1]. Reference phantoms should be accurately characterized in a manner that is laboratory and technique independent. Only a reliable characterization technique of known absolute accuracy can ensure the long term instrument standardization and data consistency required for the successful completion of a multi-center clinical trial. Characterization techniques have been mostly developed in the 1990s but interest in their absolute accuracy is more recent [3, 4, 5]. In 2005, results from the application of the MEDPHOT performance assessment protocol to a total of eight different instruments have shown inter-system variation up to 32% for μ_a and 41% for μ_s' for a given phantom [2].These results clearly demonstrate the need for advancement in the area of absolute accuracy measurement of turbid medium optical properties. Recent studies concerning liquid phantoms narrowed the intrinsic absorption and scattering coefficient agreement within 2% [4,5]. Unfortunately, liquid phantoms are not stable over the long term, and a permanent accessibility to the calibration apparatus is required to work with them. Solid phantoms such as those based on polyurethane preparation with TiO_2 particles [7] are very stable and provides a more interesting tool for in-vivo spectroscopic and imaging instrumentation development.

Measurement of time resolved transmittance [6] of light pulse through the phantoms sample has been selected as our preferred characterization method. The availability of broad spectrum supercontinuum sources now makes it possible to use the technique over a very large continuous wavelength range with high optical power. The technique produces a information rich measurement vector where problematic symptoms such as light leakage can easily be detected. The choice of transmittance geometry is also motivated by accuracy. Transmittance geometry makes it easier to isolate the unwanted light to reach the detector. In diffuse reflectance geometry, light can escape the sample close to the source fiber, reflect on surfaces, re-enter the sample close to detection and contribute to the measured trace in a substantial way. Light baffling can eliminate this flaw but is not trivial when the highest level of accuracy is desired. Finally, the technique's only calibration step is a measurement of the instrument response function. This paper presents an error analysis of the time resolved transmittance (TRT) optical properties characterization technique.

2. CHARACTERIZATION TECHNIQUE

2.1 Experimental setup

Figure 1 shows the experimental setup used to measure the time resolved transmittance of the phantoms. A super-continuum laser (Fianium, UK) was filtered to obtain a 660nm beam of 90ps pulses directed at the center of the phantom surface. Light exiting the phantom on the opposite side was collected with a MCPPMT (R3809, Hamamatsu, Japan). Time point spread functions (TPSF) were measured using a Time Correlated Single Photon Counting system (SPC-730, Becker & Hickl, Germany). The Instrument Response Function (IRF) was measured with no sample and a piece of thin (< 50 μm) translucent adhesive tape to diffuse the light over the total area of the detector.
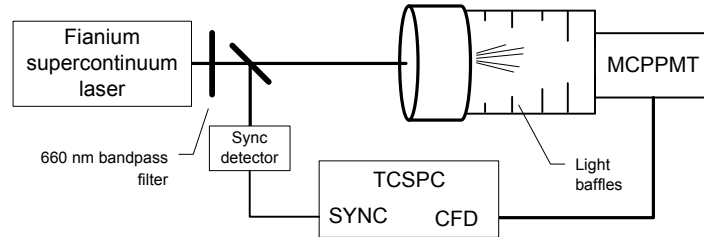

Figure 1: Experimental setup for Time resolved transmittance measurement. Reference measurements are acquired by replacing the sample by a thin diffusive tape.

2.2 Data analysis

A Monte-Carlo based model was developed based on Wang's MCML [8] with modifications to include time resolution and lateral boundaries. Fitting the data with a radiative transfer equation based model avoids any bias that could be induced by the diffusion approximation [3]. The prohibitive computation time constrains imposed by Monte-Carlo modeling were circumvented by pre-computing a TPSF database for a range of μ_s' values with zero absorption. The forward model called by the Levenberg-Marquardt fitting algorithm interpolates between the TPSF database for intermediate μ_s' and add the effect of absorption with a temporal exponential decay exploiting the fact that at a given time all photons have travelled the same distance.

A very important correction is needed to reflect the arrival time difference between the IRF measurement and the TPSF measurement. An ideal IRF measurement would position the detector at the entrance surface of the phantom since time zero is defined when the pulse hit this surface. In practice the detector is left to a fixed position and a correction must be performed by shifting the IRF vector by the time value corresponding to the time of flight of light across the thickness of the phantom to be measured.

Free fitting parameters were kept to an absolute minimum to avoid any uncontrolled bias to be compensated for by an unnecessary parameter. The time base of the measurement and the model were brought together by convoluting the modeled data vector with the IRF vector in the fitting procedure. The remaining fitting parameters are the signal amplitude and the unknown optical properties of the phantom. A very stringent fitting window was selected as anything above 1% of the peak amplitude. Figure 2 shows a typical fit result. Unless otherwise stated, the phantom nominal optical properties of the samples used for this error analysis study were $\mu_a = 0.1\,\mathrm{cm}^{-1}$ and $\mu_s' = 10\,\mathrm{cm}^{-1}$.
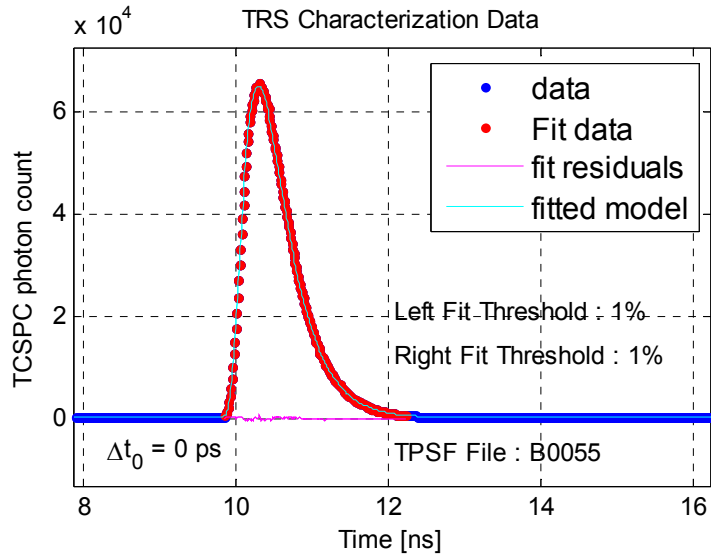
Figure 2: Typical fit results

3. RANDOM ERROR ANALYSIS

3.1 Measurement noise

Short term random fluctuations in a measured TCSPC trace come from the shot noise associated with the optical signal itself and dark counts. Measurement noise can be modeled but an experimental determination is more straightforward and convincing. The effect of measurement noise was therefore estimated by measuring four TPSF traces in sequence for six different samples. The averaged standard deviation of the fitted optical properties for each sample were $\Delta\mu_a = 0.0006\,\mathrm{cm}^{-1}\,(0.6\%)$ and $\Delta\mu_s' = 0.027\,\mathrm{cm}^{-1}\,(0.3\%)$.

3.2 Instrument response function stability

The previous section covered the contribution of fast random fluctuations that occurs on the time scale of the measurement time or faster. Slow drift of the system response can also occur. The contribution of those slow drift has been determined by analyzing a single TPSF trace with instrument response functions acquired over a 4 hours time period (see Figure 3). Standard deviation of the fitted optical properties gives $\Delta\mu_a = 0.0006\,\mathrm{cm}^{-1}\,(0.6\%)$ and $\Delta\mu_s' = 0.048\,\mathrm{cm}^{-1}\,(0.5\%)$.
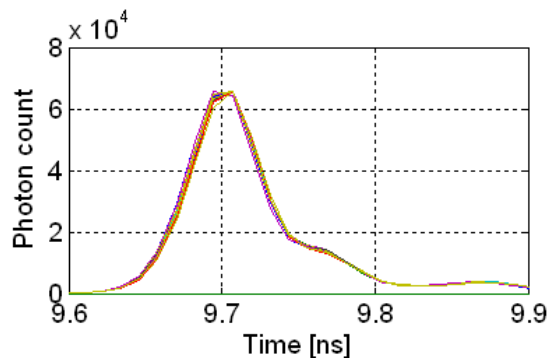

Figure 3: Instrument response functions acquired over a four hours time period

4. PHYSICAL PARAMETER UNCERTAINTY

In addition to the optical properties, the light propagation in the sample is affected by the following additional parameters: material refractive index n, thickness s and anisotropy factor g. Errors in the measured or estimated values of these parameters will translate into systematic errors in the retrieved optical properties.

4.1 Refractive index uncertainty

The refractive index of our polymer matrix was determined by a time of flight experiment. The polyurethane mix was prepared and cast into a cylindrical mold to form a clear rod. TPSF were measured with and without the rod in place. Arrival time of the pulses was determined as the point where the intensity reaches 1% of its maximal value. A low threshold was chosen to assign the arrival time to the earlier photon in order to make the result insensitive to the small broadening effect of the residual scattering of the polyurethane. Once the retardation Δt of the light induced by the rod has been determined, the refractive index is given by:

$$n = 1 + \Delta t \frac{c}{L}, \qquad (3)$$

where c is the speed of light in vacuum and L is the length of the rod. The rod length of 28.97 ± 0.03 cm generated a 0.50 ± 0.005 ns delay for a refractive index of $n = 1.521 \pm 0.006$.

The impact of this refractive index uncertainty on the retrieved optical properties uncertainty was evaluated by fitting the same experimentally measured TPSF with the nominal 1.521 refractive index value and the upper error bound 1.527. A diffusion approximation model was used for this analysis because it allows easy variation of the refractive index. The difference between the fitted optical properties for each refractive index value gives $\Delta \mu_a = 0.001\,\mathrm{cm}^{-1}\,(1\%)$ and $\Delta \mu_s' = 0.048\,\mathrm{cm}^{-1}\,(0.5\%)$.

4.2 Sample thickness uncertainty

Our characterization technique is base on pre-computed TPSF traces from a Monte-Carlo model. This TPSF database assumes a nominal sample thickness of 20mm. Real life sample varies in thickness by approximately 200µm. An experimental TPSF trace was fitted with a diffusion approximation slab model for the correct sample thickness ($t = 20\,mm$) and the erroneous sample thickness ($t = 20.2\,mm$). The difference between the fitted optical properties for each sample thickness value gives $\Delta \mu_a = 0.0009\,\mathrm{cm}^{-1}\,(0.9\%)$ and $\Delta \mu_s' = 0.15\,\mathrm{cm}^{-1}\,(1.5\%)$.

5. SYSTEMATIC ERROR ANALYSIS

5.1 TCSPC time base calibration

The time axis of a TCSPC trace is determined by the system's time-to-analog (TAC) converter. This electronics component internal to the TCSPC system measures the time between a photon detection event and a reference synchronization pulse. It is calibrated at factory by sending pulses with known delays between the CFD (detector) input and the synchronization input using a delay generator. The calibration error of this time base is estimated to 1% according to the manufacturer. The effect of this uncertainty in the time to the uncertainty in the retrieved optical properties has been estimated by using a stretched version $t' = 1.01 \cdot t$ of the time axis vector for computing the theoretical TPSF from the Monte-Carlo model. The stretching of the axis resulted in offsets of $\Delta \mu_s' = 0.091\,\mathrm{cm}^{-1}\,(0.9\%)$ and $\Delta \mu_a = 0.0015\,\mathrm{cm}^{-1}\,(1.5\%)$ in the optical properties.

5.2 Fitted model validity

Achieving optimal accuracy requires a proper model that avoids any unnecessary approximation and accurately represents the experimental conditions. Near perfect agreement between the model and the experimental data is in no way a guarantee of model validity. To explore the contribution of the model validity to the uncertainty on the optical properties we designed and experiment to challenge our characterization technique with small samples of varying geometries for which boundary effect cannot be neglected. A dedicated phantom set was fabricated for this experiment. Two phantom preparation batches of equal TiO2 concentrations but different dye concentrations were cast into molds and machined into cylinders and rectangular blocks for a total of six different geometries. Dedicated TPSF databases were computed for the analysis of each geometry. Table 1 shows the compilation of all the characterization results. CYL5520 and CYL5520bis samples are identical in size but were poured respectively first and last in their mold to verify batch uniformity. The highest relative variability, expressed as the standard deviation of the values over the mean value, is observed for the μ_a results of the low absorption set. Most of this variation is correlated to the sample thickness (variability drops from 5.97% to 1.28% if CYL5510 and CYL5530 data are omitted).

Table 1: Characterization results for the various sample geometry

geometry	size mm	thickness mm	Batch A		Batch B	
			Mu_a 1/cm	Mu_sp 1/cm	Mu_a 1/cm	Mu_sp 1/cm
CYL5510	55	10	0.0596	9.0636	0.146	8.829
CYL5520	55	20	0.0691	9.2816	0.161	9.156
CYL5530	55	30	0.0709	9.4989	0.164	9.317
REC3020	30	20	0.0715	9.4902	0.162	9.321
REC5020	50	20	0.0696	9.4517	0.163	9.354
REC8020	80	20	0.0702	9.4600	0.159	9.186
CYL5520bis	55	20	0.0701	9.4965	0.162	9.477
		Mean	0.069	9.39	0.159	9.23
		Std dev.	4.10E-03	0.16	5.99E-03	0.21
		Percent variation	**5.97%**	**1.74%**	**3.76%**	**2.26%**

6. CONCLUSION

The various error sources estimated in this work are compiled in Table 2. Worst case values were selected for the model validity contribution. A 2 sigma root mean square sum of all contributor gives uncertainties of $\Delta\mu_a|_{2\sigma} = \pm 0.009\,\text{cm}^{-1}\,(9\%)$ and $\Delta\mu_s'|_{2\sigma} = \pm 0.5\,\text{cm}^{-1}\,(5\%)$. Measurement noise and IRF stability could be brought down with averaging multiple measurements. The sample thickness contribution could be reduced by tighter manufacturing tolerances on the sample thickness. Sample thickness can be measured with a much high accuracy. A 2 parameter TPSF database that could interpolate for a measured sample thickness in addition to the scattering coefficient would also be very effective in reducing this contribution. A more accurate determination of the index of refraction could be performed with a longer interaction length. The timebase calibration accuracy could be verified with a time of flight experiment similar to the one described in section 4.1 but using a rod of glass with known refractive index. Refractive index can be characterized with an accuracy of $2\cdot 10^{-4}$ and the length of a 30 cm rod can be measured with a similar accuracy. This accuracy would transfer to the predicted time of flight that would then serve as a reference to adjust the time axis of the TCSPC system. The largest contributor is by far the model inaccuracy and will be the focus of future effort. Improvement in this contributor is not trivial. Foreseeable bias sources such as boundary effect, sample thickness correction and RTE modeling have already been taken into account. The sample geometry experiment provides a measure of its symptom that will serve to investigate the root cause of this remaining bias.

Table 2: Error budget compilation. Relative values are computed according to the nominal $\mu_a = 0.1\,cm^{-1}$, $\mu'_s = 10\,cm^{-1}$ optical properties.

	Absolute error (cm^-1)		Relative error (%)	
	µa	µs'	µa	µs'
Measurement noise	0.0006	0.027	0.60%	0.27%
IRF stability	0.0006	0.05	0.60%	0.50%
Sample thickness error	0.0009	0.15	0.90%	1.50%
Refractive index error	0.001	0.048	1.00%	0.48%
Time base calibration	0.0015	0.091	1.50%	0.91%
Model inaccuracy	0.004	0.16	4.00%	1.60%
1 sigma RSS sum	**0.005**	**0.25**	**4.56%**	**2.49%**
2 sigma RSS sum	**0.009**	**0.50**	**9.12%**	**4.98%**

REFERENCES

[1] Pogue, B. W., Patterson, M. S., "Review of tissue simulating phantoms for optical spectroscopy, imaging and dosimetry," J. Biomed. Opt. 11(4), 041102 (2006).

[2] Pifferi, A., Torricelli, A., Bassi, A., Taroni, P., Cubeddu, R., Wabnitz, H., Grosenick, D., Moller, M., Macdonald, R., Swartling, J., Svensson, T., Andersson-Engels, S., van Veen, R. L. P., Sterenborg, H. J. C. M., Tualle, J.-M., Nghiem, H. L., Avrillier, S., Whelan, M., Stamm, H., "Performance assessment of photon migration instruments: the MEDPHOT protocol," Appl. Opt. 44(11), 2104-2114 (2005).

[3] Alerstam, E., Andersson-Engels, S., Svensson, T., "Improved accuracy in time-resolved diffuse reflectance spectroscopy" Opt. Express 16(14), 10434-10448 (2007).

[4] Spinelli, L., Martelli, F., Farina, A., Pifferi, A., Torricelli, A., Cubeddu, R., Zaccanti, G., "Calibration of scattering and absorption properties of a liquid diffusive medium at NIR wavelengths. Time-resolved method," Opt. Express 15(11), 6589-6604 (2007).

[5] Martelli, F., Zaccanti, G., "Calibration of scattering and absorption properties of a liquid diffusive medium at NIR wavelengths. CW method," Opt. Express 15(2), 486-500 (2007).

[6] Patterson, M. S., Chance, B., Wilson, B. C., "Time resolved reflectance and transmittance for the non-invasive measurement of tissue optical properties," Appl. Opt. 28, 2331-2336 (1989).

[7] Vernon, M. L., Fréchette, J., Painchaud, Y., Caron, S., Beaudry, P., "Fabrication and characterization of a solid polyurethane phantom for optical imaging through scattering media," Appl. Opt. 38(19), 4247-4251 (1999).

[8] Wang, L.-H., Jacques, S. L., Zheng, L.-Q., "MCML – Monte Carlo modeling of photon transport in multi-layered tissues," Computer Methods and Programs in Biomedicine 47, 131-146 (1995).